Electrocatalysis (2015) 6:51–59
DOI 10.1007/s12678-014-0216-z

On the Temperature Dependence of Hydrogen Evolution Reaction at Nickel Foam and Pd-Modified Nickel Foam Catalysts

Boguslaw Pierozynski · Tomasz Mikolajczyk

Published online: 17 July 2014

Abstract This communication reports on hydrogen evolution reaction (HER), studied at Ni foam and Pd-activated nickel foam materials in 0.1-M NaOH solution over the temperature range of 20–60 °C. Catalytic modification of Ni foam leads to significant facilitation of temperature-dependent HER kinetics, manifested through radically reduced values of charge-transfer resistance parameter, as well as substantially modified Tafel polarization curves. The presence of a catalytic additive (Pd) is evidenced through scanning electron microscopy (SEM) analysis.

Keywords Nickel foam · Catalytic modification · HER · Electrochemical impedance spectroscopy

Introduction

Cathodic evolution of hydrogen at metal electrodes is one of the most significant electrochemical processes, especially important with respect to rapid development of proton exchange membrane (PEM) fuel cell and battery technologies. On the other hand, nickel makes one of the best non-noble catalyst materials suitable for hydrogen evolution reaction (HER) in alkaline media, primarily due to its high corrosion resistance at high pH values [1-5]. Nickel foams are made by chemical vapour deposition (CVD) [6], or electrochemical or electroless deposition method, typically with a polyurethane foam precursor [7]. Such-produced catalyst is characterized by high porosity and specific surface area, and also by good electrical conductivity, high corrosion resistance and superior mechanical properties [7, 8]. Significant improvement of electrocatalytic properties of bare nickel foam (e.g. towards HER or oxidation of aliphatic alcohols) could be realized through surface deposition of nano-structured noble metals (e.g. Pd, Ru, Rh, Pt or their binary/ternary alloys). The above might be performed by means of electrodeposition, spontaneous deposition [8-10] or by chemical reduction processes, where the latter are typically facilitated with $NaBH_4$, ethylene glycol, hydrazine or their compositions [11-15].

In this communication, Pd-activated nickel foam catalyst material was prepared via spontaneous deposition method [8], to produce cathode having superior HER performance for alkaline environments. The choice of palladium results from the fact that Pd element itself is well known to exhibit high electrochemical activity towards hydrogen absorption and evolution processes [16-21] with an exchange current density value of 1×10^{-3} A cm^{-2}, which is very close to that exhibited by Pt [18]. These properties of palladium along with highly porous, large surface area metallic Ni foam structure [22] make a Pd-modified nickel foam composite material a very good candidate for studying the HER behaviour.

Experimental

All solutions were prepared by means of a Direct-Q 3 UV ultra-pure water purification system from Millipore (18.2 MΩ cm water resistivity). A 0.1-M NaOH supporting solution was prepared from AESAR, 99.996 % NaOH pellets. An electrochemical cell, made of Pyrex glass, was used during the course of this work. The cell comprised three electrodes: a Ni-foam-based working electrode (WE) in a central part, a reversible Pd (0.5-mm-diameter wire of 99.9 % purity, Aldrich)

B. Pierozynski (✉) · T. Mikolajczyk
Department of Chemistry, Faculty of Environmental Management and Agriculture, University of Warmia and Mazury in Olsztyn, Plac Lodzki 4, 10-957 Olsztyn, Poland
e-mail: bogpierozynski@yahoo.ca

B. Pierozynski
e-mail: boguslaw.pierozynski@uwm.edu.pl

hydrogen electrode (RHE) as reference and a Pt (1.0-mm-diameter wire of 99.9998 % purity, Johnson Matthey, Inc.) counter electrode (CE), both placed in separate compartments. The procedures for cleaning the cell and preparation of the CE/RHE electrodes for the measurements were as previously described in Pierozynski and Smoczynski [23], Pierozynski [24] and Pierozynski [25]. Before conducting the HER experiments, each Ni foam electrode was also activated in 0.1 M NaOH by cathodic polarization, carried out at 20 mA for 300 s in order to maintain surface area reproducibility [26].

Nickel foam was supplied by MTI Corporation (>99.99 % Ni, thickness 1.6 mm, surface density 346 g m^{-2}, porosity ≥95 %). All electrodes were 1 cm× 1 cm, for which pure Ni foam accounted for about 2.6 cm^2 of geometrical area and 0.030 g (~88 cm^2 g^{-1}). Spontaneous deposition of Pd catalyst on nickel foam samples was performed according to the corresponding description given in Verlato et al. [8]. Hence, freshly cut foam samples were subjected to acetone and CH_2Cl_2 wash (15 min+ultrasonication), following air drying and acid etching in 2 M HCl (15 min at 60 °C). Then, spontaneous deposition of metal catalyst was realized by dipping pretreated foam electrodes in 0.005 M $PdCl_2$ (pH 1.0, $t_{dep.}$=15–300 s, temperature 25±1 °C) to produce Pd-activated Ni foam catalyst material. Working electrode assemblies were made by mechanically attaching Ni foam/Pd-modified Ni foam samples to 0.5-mm-diameter Ni wire (Aldrich, ≥99.9 %). In addition, shrinkable PE or PTFE sleeves were used to provide Pd wire insulation within the electrochemical cell.

A.c. impedance spectroscopy and quasi steady state polarization techniques were employed during the course of this work. All measurements were performed over the temperature range of 20–60 °C (controlled by laboratory water bath) by means of the *Solartron* 12,608 W Full Electrochemical System, consisting of 1260 frequency response analyser (FRA) and 1287 electrochemical interface (EI) for an a.c. signal of 5 mV and the frequency range sweep between 1.0×10^{5} and 0.5×10^{-1} Hz. The instruments were controlled by *ZPlot 2.9* or *Corrware 2.9* software for Windows (Scribner Associates, Inc.), whereas data analysis was performed with *ZView 2.9* (*Corrview 2.9*) software package. The impedance spectra were fitted by means of a complex, non-linear, least squares immitance fitting program, *LEVM 6*, written by J.R. Macdonald [27]. In addition, quasi-potentiostatic cathodic polarization experiments (recorded at a scan rate of 0.5 mV s^{-1}) for the HER were carried out at all examined Ni foam electrodes. Also, an appropriate correction was introduced [28], in order to account for a small but significant temperature shift of the Pd RHE over the studied temperature range of 20–60 °C.

Spectroscopic characterization of Pd-activated Ni foam electrodes was performed by means of Quanta FEG 250 scanning electron microscope (SEM). In addition, powder X-ray diffraction (XRD) technique was employed to determine average size of Pd crystallite domains for the selected Pd-modified Ni foam samples. The XRD spectra were recorded by means of Siemens D500 powder diffractometer with Cu K_α radiation (λ= 1.5418 Å, *U*=38 kV, *I*=30 mA) in a standard Bragg-Brentano mode without sample spinning. Experimentally recorded data were analysed by means of the phase analysis XRAYAN software.

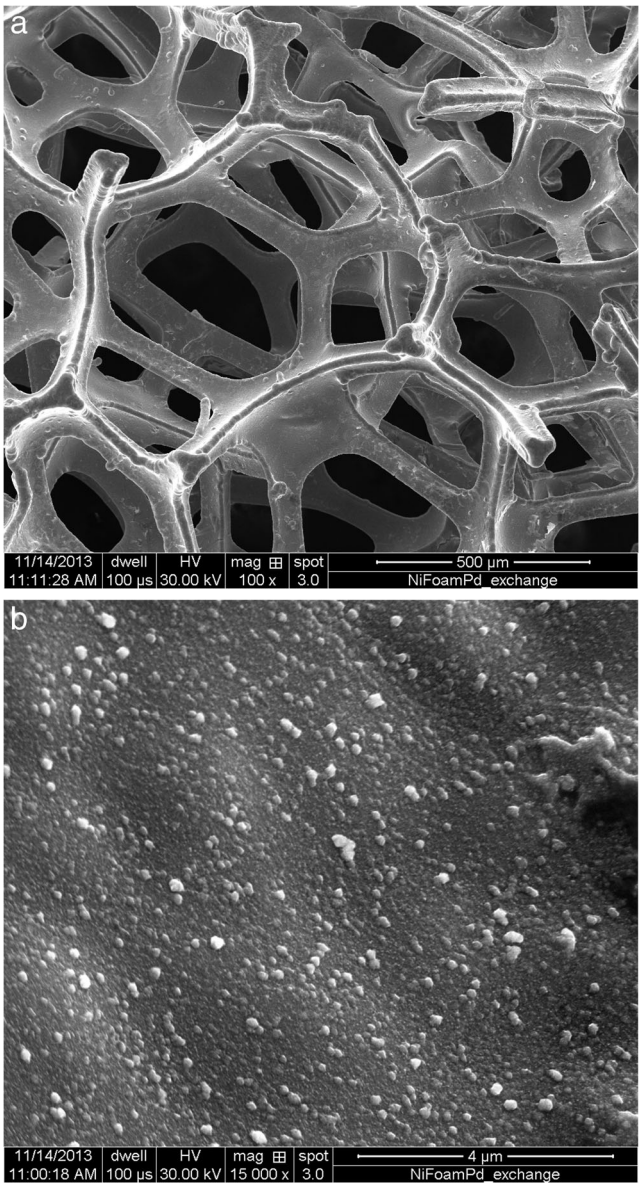

Fig. 1 **a** SEM micrograph picture of Pd-modified Ni foam surface (~0.1 wt% Pd), taken at×100 magnification; **b** As in Fig. 1a, but taken at×15,000 magnification

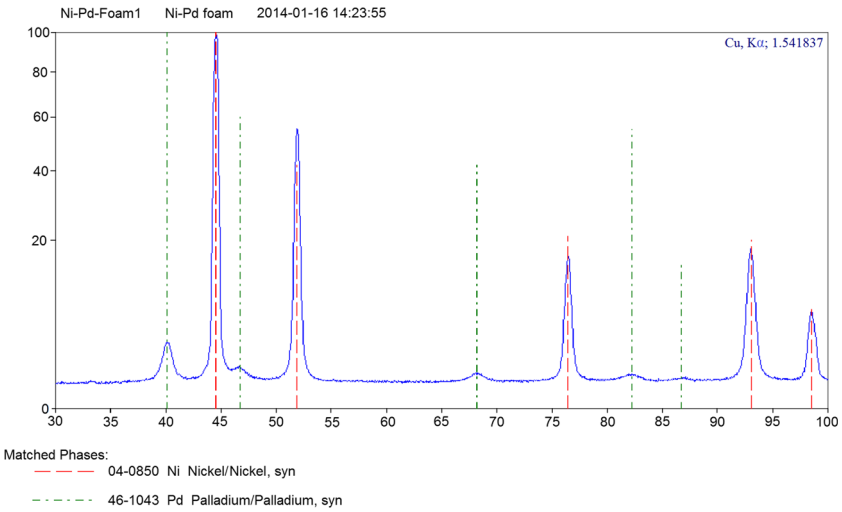

Fig. 2 XRD pattern for spontaneously deposited Pd element on nickel foam substrate, where observed diffraction lines correspond to the following sequence of fcc indices: (111), (200), (220), (311) and (222) for both Ni and Pd elements

Results and Discussion

SEM and XRD Characterizations of Pd-Modified Ni Foam Electrode

Figure 1a, b illustrates the effect of spontaneous deposition of palladium at a very low level (~0.1 wt% Pd) on the MTI foam, recorded for the magnifications of×100 and× 15,000, respectively. Hence, at the magnification of× 15,000, high-density and homogeneously distributed small Pd nuclei could clearly be seen in Fig. 1b. The SEM-approximated Pd grain size value came to 10.0± 1.0 nm. The above was performed through utilization of the *Image Analysis Program* (NIS-Elements Basic Research on Nikon), based on an analogous procedure to that described in detail in Smoczyński et al. [29]. In addition, the powder-XRD-calculated average Pd grain size value came to 7.0±0.7 nm (see Fig. 2 above). Measurements were carried out based on the Scherrer's method, which correlates the size of crystallite domains with relative widening of diffraction peaks (see Pecharsky and Zavalij [30] for further details).

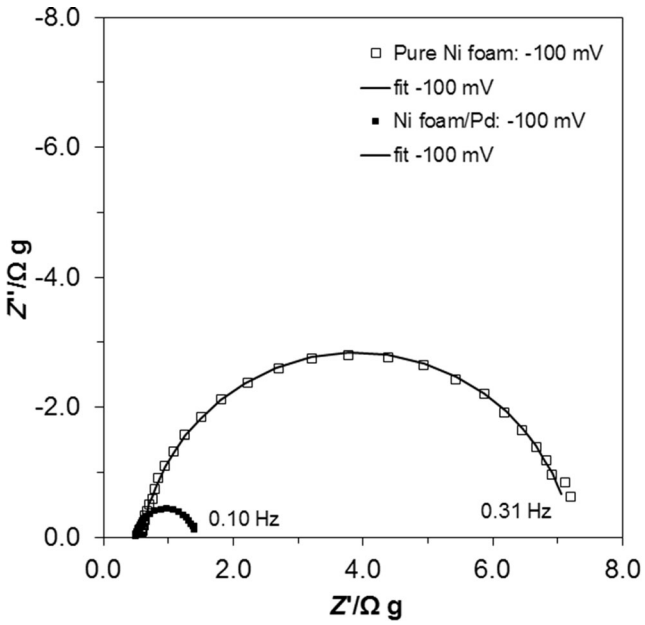

Fig. 3 Complex-plane impedance plots for the HER on pure and Pd-modified Ni foam electrode surfaces in contact with 0.1 M NaOH, recorded at room temperature for −100 mV (vs RHE). The *solid lines* correspond to representation of the data according to the equivalent circuit shown in Fig. 4

A.c. Impedance Behaviour of HER on Pure and Pd-Modified Ni Foam Materials in 0.1 M NaOH

A.c. impedance characterization of the HER on pure Ni foam and catalyst (Pd)-modified Ni foam electrodes in 0.1 M NaOH is shown in Fig. 3 and Tables 1, 2 and 3. Hence, the impedance-examined, both unmodified and Pd-activated Ni foam electrodes exhibited single, "depressed" semicircles (a single-step charge-transfer reaction) at all examined potentials and reaction temperatures, in the explored frequency range (please note that a high-frequency semicircle electrode porosity response, which is typically observed in alkaline media, was practically indiscernible). Examples of Nyquist impedance plots, recorded for pure and the Pd-modified nickel foam electrodes at −100 mV versus RHE, are shown in Fig. 3 below. The overpotential dependence of Faradaic reaction resistance (R_{ct}) and double-layer capacitance (C_{dl}) parameters for the HER, examined over the temperature range of 20–60 °C at pure nickel foam (derived based on a constant phase element (CPE)-modified Randles equivalent circuit model shown in Fig. 4) is presented in Table 1. The CPE element was used in the circuit in order to account for the capacitance dispersion [31, 32] effect, represented by somewhat distorted semicircles in the Nyquist impedance plots.

Table 1 Electrochemical parameters for the HER on cathodically activated pure Ni foam electrode in contact with 0.1 M NaOH, studied over the temperature range of 20–60 °C

E/mV	R_{ct}/Ω g				
	20 °C	30 °C	40 °C	50 °C	60 °C
−50	13.653±0.066	3.759±0.037	1.822±0.014	1.226±0.009	0.844±0.007
−100	6.674±0.022	3.134±0.011	1.439±0.006	0.939±0.004	0.761±0.004
−150	2.353±0.012	1.653±0.008	0.757±0.004	0.556±0.003	0.496±0.003
−200	0.877±0.008	0.777±0.004	0.391±0.003	0.311±0.002	0.317±0.002
−250	0.464±0.008	0.402±0.003	0.236±0.003	0.207±0.003	0.216±0.002
−300	0.289±0.005	0.248±0.002	0.171±0.003	0.155±0.003	0.149±0.003
−350	0.209±0.005	0.187±0.004	0.143±0.004	0.121±0.003	0.120±0.003
−400	0.162±0.003	0.141±0.003	0.107±0.002	0.097±0.002	0.089±0.002
	C_{dl}/μF $g^{-1}s^{\varphi 1-1}$				
−50	10,959±104	10,316±227	10,262±267	11,852±374	11,959±379
−100	8,608±81	8,694±118	8,371±201	8,319±181	10,125±264
−150	6,545±157	6,771±158	6,348±221	6,520±268	8,363±345
−200	4,931±256	5,560±183	5,049±243	5,048±316	6,726±242
−250	5,019±501	4,914±259	4,436±375	4,958±510	6,568±523
−300	4,011±445	4,570±352	4,371±516	5,274±654	5,614±666
−350	3,680±596	5,350±779	7,376±1,134	6,068±892	9,690±1,308
−400	3,806±495	4,544±680	5,166±607	5,448±591	5,668±939

The results were obtained by fitting the CPE-modified Randles (Fig. 4) equivalent circuit to the experimentally obtained impedance data (reproducibility usually below 5 %, $\chi^2 = 3\times10^{-4}$ to 2×10^{-3})

Table 2 Electrochemical parameters for the HER on Pd-modified Ni foam electrode in contact with 0.1 M NaOH, studied over the temperature range of 20–60 °C

E/mV	R_{ct}/Ω g				
	20 °C	30 °C	40 °C	50 °C	60 °C
−50	1.526±0.013	0.310±0.006	0.273±0.007	0.195±0.003	0.151±0.002
−100	0.928±0.007	0.373±0.005	0.284±0.003	0.198±0.001	0.156±0.001
−150	0.564±0.004	0.344±0.006	0.253±0.006	0.175±0.002	0.143±0.003
−200	0.370±0.003	0.258±0.003	0.209±0.003	0.150±0.001	0.128±0.002
−250	0.263±0.003	0.199±0.003	0.170±0.002	0.129±0.002	0.115±0.002
−300	0.198±0.003	0.154±0.002	0.135±0.002	0.108±0.001	0.102±0.002
−350	0.157±0.003	0.126±0.003	0.112±0.003	0.095±0.001	0.094±0.004
−400	0.128±0.002	0.105±0.002	0.095±0.001	0.080±0.001	0.078±0.001
	C_{dl}/μF g^{-1} $s^{\varphi 2-1}$				
−50	204,554±2,577	283,856±14,760	303,933±13,038	229,245±11,920	217,082±11,288
−100	188,395±2,826	216,844±7,372	197,812±6,329	178,624±5,680	191,293±8,225
−150	168,942±3,209	195,436±8,403	202,904±12,782	174,723±10,133	183,216±15,023
−200	166,952±4,340	192,497±6,737	190,181±7,797	174,156±7,662	161,856±8,254
−250	157,458±5,983	182,805±9,652	187,070±10,288	184,273±11,424	167,292±11,041
−300	157,822±9,153	169,185±9,474	171,439±10,252	181,095±13,401	189,936±18,993
−350	166,592±14,660	171,318±16,446	182,083±16,933	154,350±13,274	246,764±39,482
−400	162,506±10,563	186,372±14,350	177,697±12,972	157,085±11,153	182,815±14,076

The results were obtained by fitting the CPE-modified Randles (Fig. 4) equivalent circuit to the experimentally obtained impedance data (reproducibility usually below 5 %, $\chi^2 = 1\times10^{-4}$ to 3×10^{-3})

Table 3 Exchange current density, Tafel slope and activation energy electrochemical parameters for the HER, obtained on pure Ni foam and Pd-modified Ni foam electrodes in contact with 0.1 M NaOH over the temperature range of 20–60 °C

Pure Ni foam					
Parameter	20 °C	30 °C	40 °C	50 °C	60 °C
j_o/A cm^{-2}					
A.c. impedance:	1.2×10^{-6}	–	–	–	2.0×10^{-5}
Tafel plots:	9.8×10^{-7}	2.3×10^{-6}	4.6×10^{-6}	7.7×10^{-6}	1.2×10^{-5}
b_c/mV dec^{-1}	−137	−169	−183	−193	−222
	−100 mV	−200 mV	−300 mV	−400 mV	
E_A/kJ mol^{-1}	45.4	24.1	14.6	12.7	
Pd-modified Ni foam					
	20 °C	30 °C	40 °C	50 °C	60 °C
j_0/A cm^{-2}					
A.c. impedance:	1.3×10^{-5}	–	–	–	1.4×10^{-4}
Tafel plots:	8.6×10^{-6}	1.1×10^{-5}	1.7×10^{-5}	2.1×10^{-5}	5.3×10^{-5}
b_c/mV dec^{-1}	−65	−76	−74	−79	−97
	−100 mV	−200 mV	−300 mV	−400 mV	
E_A/kJ mol^{-1}	34.3	21.6	13.6	10.2	

Thus, for the cathodically activated Ni foam electrodes, the recorded R_{ct} parameter examined at 20 °C decreased from 13.653 Ω g at −50 mV to 0.162 Ω g at the potential of −400 mV versus RHE. Simultaneously, the C_{dl} parameter significantly reduced from 10,959 to 3,806 μF g^{-1} s$^{\varphi 1-1}$ (2.9 times) for the same potential range. The latter effect most likely results from partial blocking of electrochemically active electrode surface by freshly formed H_2 bubbles. The above might easily be visualized for a complex Ni foam electrode structure (Fig. 1a, b), especially at significant overpotentials. Also, when the capacitance value of 10,959 μF g^{-1} s$^{\varphi 1-1}$ (recorded for electrode weight of 35.0 mg at −50-mV RHE) is referred to that commonly used value of 20 μF cm^{-2} in literature for smooth and homogeneous surfaces [33, 34], electrochemically active surface area of the Ni foam electrode could roughly be estimated at 19.2 cm^2 (or 548 cm^2 g^{-1}). Similar impedance behaviour (with a single-step charge-transfer process) has recently been presented by Grden et al. [35] for the HER characterization of Incofoam® Ni foam commercial product in 0.5-M KOH solution. There, the recorded at −200-mV R_{ct} parameter value for an etched foam sample came to 43 Ω (~1.30 Ω g), which is significantly higher than 0.877 Ω g recorded for analogous conditions in Table 1. Simultaneously, the impedance-approximated [35] specific surface area for the etched Incofoam® sample came to 241 cm^2 g^{-1}, as compared to that of 548 cm^2 g^{-1} for the MTI foam examined in this work. These results suggest that the latter nickel foam provides significantly enhanced electrochemical properties towards the HER (most likely due to its unique porous structure), as compared to the former one. In another recent work by van Drunen et al. [36], cyclic-voltammetry-derived values of electrochemically active surface area for analogous Ni foam material were on the order of 250–450 cm^2 g^{-1}. Other important options for the fabrication of highly-porous, three-dimensional Ni or Ni-originated matrices include powder-based [37, 38] and electrochemical deposition processes [10, 39]. As all options are significant, nickel foam comparatively provides a fully commercialized technology with highly reproducible material having superior mechanical and electrical properties.

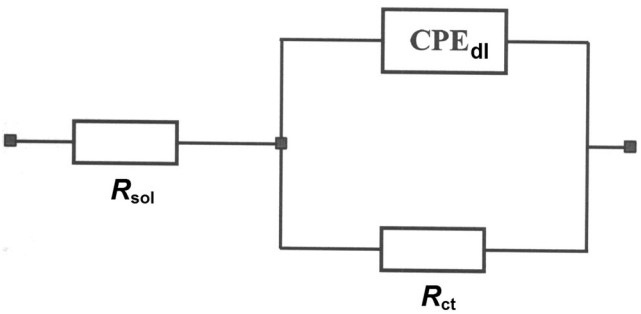

Fig. 4 Equivalent circuit model used for fitting the impedance data for both pure and Pd-modified Ni foam electrodes, obtained in 0.1 M NaOH. The circuit includes a constant phase element (CPE) for distributed capacitance; R_{ct} and C_{dl} (as CPE$_{dl}$) elements correspond to the HER charge-transfer resistance and double-layer capacitance components, and R_{sol} is solution resistance

Table 1 also presents the temperature dependence of the R_{ct} and C_{dl} electrochemical parameters, studied over the temperature range of 20–60 °C. Hence, for the two temperature extremes, 20 and 60 °C, the recorded charge-transfer resistance exhibited significant reduction, correspondingly from 13.653 to 0.844 Ω g (by 16.2 times) at −50 mV and from 0.162 to 0.089 Ω g (by 1.8 times) at −400 mV. Furthermore, the C_{dl} parameter recorded at individual overpotentials kept slowly rising upon temperature increase (see Table 1). The above could be explained in terms of extended access to the catalytic

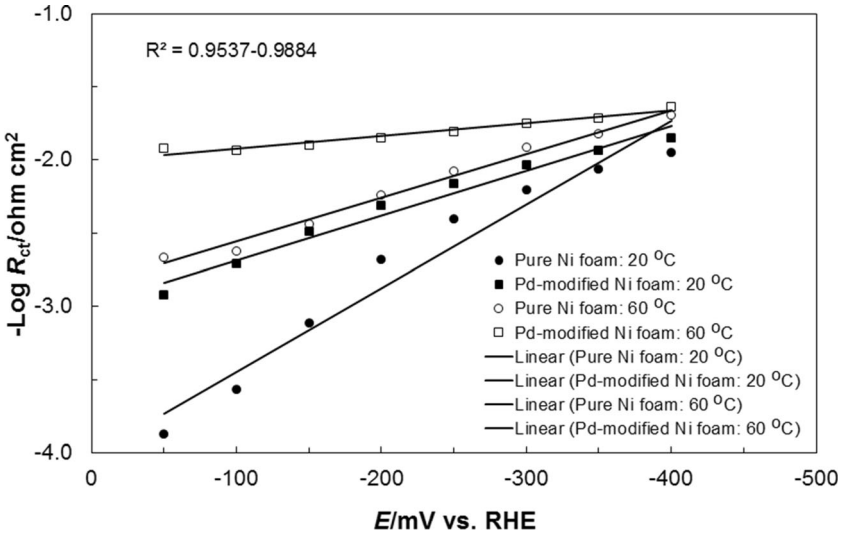

Fig. 5 Linear plots of −log R_{ct} in function of potential (vs RHE), obtained for the HER performed on pure and Pd-modified Ni foam electrodes in 0.1-M NaOH solution, recorded at 20 and 60 °C. *Symbols* represent experimental results and *lines* are data fits

surface within the porous electrode structure at elevated temperatures. In addition, higher temperatures should considerably facilitate hydrogen bubble removal.

On the other hand, the recorded charge transfer resistance parameter for the Pd-modified Ni foam electrode at 20 °C ranged from 1.526 to 0.128 Ω g for the overpotential range of 50–400-mV RHE (see Table 2). The above means considerable reduction of the R_{ct} parameter (as compared to those R_{ct} values recorded for the unmodified Ni foam surface), namely by 8.9 times and 1.3 times at −50 and −400 mV, respectively. In addition, deposition of catalytic Pd nano-structure resulted in significant enhancement of electrochemically available surface area, as compared to that of the nickel foam baseline material. Thus, for the Pd-activated Ni foam, the recorded values of the C_{dl} parameter at −50-mV RHE came to 204,554 μF g^{-1} $s^{\varphi 2-1}$ (about 10,228 cm^2 g^{-1}). The above is ~18.7 times greater than that recorded for the baseline Ni foam cathode. Understandably, for the catalyst-modified nickel foam material, the C_{dl} parameter exhibited similar (decreasing) overpotential dependence to that recorded for the baseline Ni foam electrode. However, the recorded C_{dl} ratio for the −50/−400-mV pair came to ~1.3, which was radically smaller than that recorded for the unmodified Ni foam electrode above (2.9 times). In other words, on the Pd-modified nickel foam, the HER predominantly proceeds on the catalyst-covered outer parts of the foam structure, so that the removal of hydrogen bubbles from the catalyst becomes strongly facilitated.

Correspondingly, Table 2 above shows the temperature dependence of the R_{ct} and C_{dl} parameters, examined over the temperature range of 20–60 °C for the Pd-modified Ni foam electrode. Thus, the recorded (at 20 and 60 °C) charge-transfer resistance exhibited significant reduction, respectively from 1.526 to 0.151 Ω g (by 10.1 times) at −50 mV and from 0.128 to 0.078 Ω g (by 1.6 times) at −400 mV. Then, the C_{dl} parameter recorded at specific overpotentials also continued increasing upon rising temperature (see Table 2 and compare with the corresponding results presented in Table 1 above).

Finally, dimensionless φ_1 and φ_2 parameters of the CPE circuit (see Fig. 4 and Tables 1 and 2), where φ determines the constant phase angle in the complex-plane plot, ($0 \le \varphi \le 1$) varied between 0.83–0.97 and 0.82–0.94, respectively.

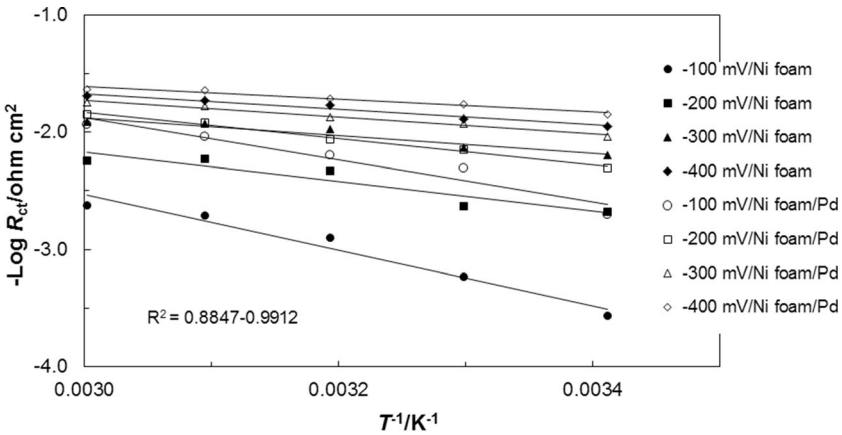

Fig. 6 Linear plots of −log R_{ct} versus T^{-1} for the HER performed on pure and Pd-modified Ni foam electrodes in 0.1-M NaOH solution, at the stated overpotential values

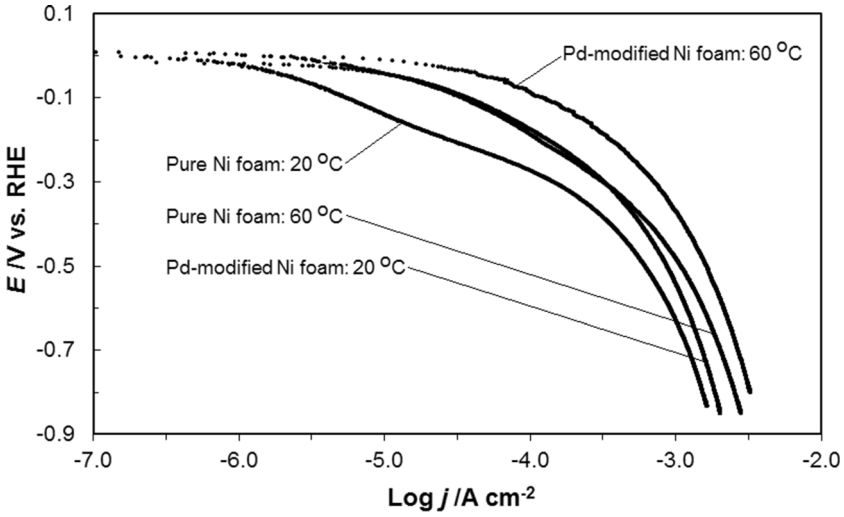

Fig. 7 Quasi-potentiostatic cathodic Tafel polarization curves (recorded at a rate of 0.5 mV s^{-1}) for the HER on pure and Pd-modified Ni foam electrode surfaces, carried out in 0.1-M NaOH solution at 20 and 60 °C (appropriate *iR* correction was made based on the solution resistance derived from the impedance measurements)

Based on the linear relationship $-\log R_{ct}$ versus overpotential (for kinetically controlled reactions), exhibited here over the overpotential range of 50–400 mV versus RHE (see Fig. 5 above), the exchange current-densities for the HER were calculated based on the Butler-Volmer equation and through utilization of the relation between the exchange current density (j_0) and the R_{ct} parameter for overpotential approaching zero value [5, 40-42]. Hence, the impedance-derived values of the j_0 parameter came to 1.2×10^{-6} A cm^{-2} (at 20 °C) and 2.0×10^{-5} A cm^{-2} (at 60 °C) for the unmodified Ni foam, whereas significantly increased j_0 values, namely, 1.3×10^{-5} A cm^{-2} (at 20 °C) and 1.4×10^{-4} A cm^{-2} (at 60 °C), were recorded for the Pd-modified nickel foam catalyst material (see Table 3 for details). The room-temperature-derived HER exchange current density value (1.3×10^{-5} A cm^{-2}) for the Pd-activated nickel foam is significantly higher than the j_0 for bulk Ni (6.3×10^{-6} A cm^{-2}), but dramatically lower than the corresponding bulk j_0 parameter value for Pd element (1×10^{-3} A cm^{-2}) [18]. However, it should be understood that electrocatalytic activity of a catalyst material strongly depends on the extent of its electrochemically active surface area and nano-structural properties. One should also note that nano-scaled catalytic structures typically demonstrate far superior electrocatalytic activities to those exhibited by the respective bulk catalyst materials. Thus, highly modifiable (e.g. by deposition of variable, but negligible amount of Pd), large surface area porous Ni foam could potentially produce exceptionally active and relatively inexpensive HER catalyst.

In addition, Fig. 6 presents $-\log R_{ct}$ versus T^{-1} Arrhenius-type plots, constructed based on the $R_{ct}=f(T)$ impedance results, presented for the overpotential range of 100–400 mV versus RHE for the pure and the Pd-activated Ni foam catalyst electrodes. Thus-obtained experimental electrochemical energies of activation, E_A [kJ mol^{-1}] for the HER on the Pd-modified nickel foam,

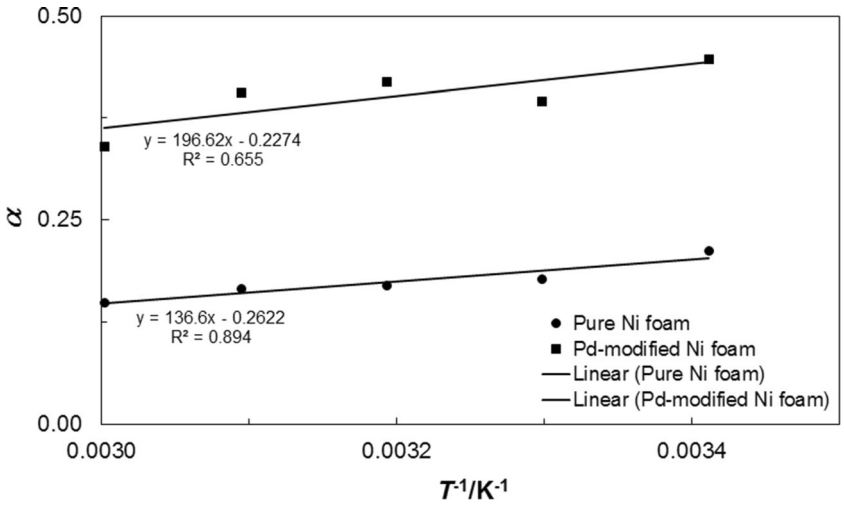

Fig. 8 Temperature dependence of experimental Tafel charge transfer coefficient for the HER on pure and Pd-modified foam electrodes in contact with 0.1-M NaOH solution

came significantly lower (by ~25 % at −100 mV and by 20 % at −400 mV) than those for the bare Ni foam electrode (Table 3).

HER Characterization by Steady State Tafel Polarization Plots

The kinetic results discussed above are in good agreement with these of the potentiostatic Tafel polarizations, presented for the pure and the Pd-modified Ni foam HER catalysts (performed at 20 and 60 °C) in Fig. 7. In fact, radical enhancement of the HER performance upon introduction of catalytic amount of Pd into Ni foam structure could clearly be observed over the kinetically controlled, low-overpotential region in this figure. The recorded cathodic Tafel slopes (parameter b_c in Table 3) exhibited significant temperature dependence (see Conway [43] for details) for both examined electrode materials. Hence, for the temperature range of 20–60 °C, the Tafel slope changed from −137 to −222 mV dec^{-1} and from −65 to −97 mV dec^{-1} for the baseline Ni foam and the Pd-modified Ni foam catalyst materials, respectively. At the same time, considerable reduction of the cathodic Tafel slope for the palladium-activated Ni foam came in-line with significant facilitation of the exchange current density parameter. Thus, the Tafel-based values of the j_0 parameter for the HER reached 9.8×10^{-7} (at 20 °C) and 1.2×10^{-5} A cm^{-2} (at 60 °C) for the unmodified Ni foam, and 8.6×10^{-6} (at 20 °C) and 5.3×10^{-5} A cm^{-2} (at 60 °C) for the Pd-modified nickel foam electrode (see other details in Table 3). These results are in a fairly good agreement with the impedance-derived values of the j_0 parameter. However, the recorded difference between the Tafel-calculated and the impedance-derived values of the exchange current density parameter in Table 3 (especially perceptible for the Pd-modified Ni foam electrode) could possibly result from somewhat inferior quality of the Tafel fit for this case. It should be stated here that all calculated in this work exchange current-densities and cathodic Tafel slopes for the HER are within the range that is commonly quoted for Ni-porous entities in literature. Hence, Dominguez-Crespo et al. have recently reported [38] Tafel slopes in the range 152–214 mV dec^{-1} and optimum j_0 value of 6.3×10^{-5} A cm^{-2} for highly porous (La, Ce)/Ni electrodes. Furthermore, Vazquez-Gomez et al. [10] reported for cathodically deposited porous Ni layer onto Ni disk electrode a Tafel slope of 138 mV dec^{-1} and a respective j_0 value equal to 3.2×10^{-4} A cm^{-2}, whereas further Ru or Ir modifications (by spontaneous metal depositions) resulted there (generally) in reduction of Tafel slopes and a dramatic increase (by 7–38 times) of the j_0 parameter (see Table 3 in Vazquez-Gomez [10] and compare with the results presented above). Similar trends for the recorded b_c and j_0 parameters (including their temperature dependence) were also reported [39] for three-dimensional porous Ni structures, fabricated over the so-called double-template electrochemical deposition process (see Table 2, Herraiz-Cardona [39]).

In addition, as originally argued by Conway [43] (based on non-linear T dependence of the b_c Tafel slope), the recorded charge transfer coefficient α linearly decreased with rising temperature [44] for both examined HER catalyst materials (see Fig. 8 above).

Conclusions

Palladium nano-deposit (at ~0.1 wt%) on the surface of cathodically activated Ni foam material significantly enhanced catalytic activity of baseline foam material towards cathodic evolution of hydrogen in 0.1-M NaOH solution. The above was specifically observed over kinetically controlled, low-overpotential range, being a result of superior HER activity of a catalytic Pd additive, in addition to the resultant, extensive modification of electrochemically active surface for this catalyst material.

Both Tafel slopes, as well as charge transfer coefficient, exhibited temperature-dependent behaviour. Significant facilitation of the HER performance for the Pd-modified Ni foam material was revealed through considerably reduced Tafel slopes and electrochemical energies of activation, and by substantially increased values of exchange current density parameter, as compared to those obtained for the unmodified nickel foam cathode. Finally, the results obtained in this work indicated substantial opportunities for Ni-foam-modified cathode materials in commercial alkaline water electrolysers.

References

1. B.E. Conway, B.V. Tilak, Adv. Catal. **38**, 1 (1992)
2. J.Y. Huot, L. Brossard, Int. J. Hydrog. Energy **12**(12), 821 (1987)
3. H.E.G. Rommal, P.J. Morgan, J. Electrochem. Soc. **135**(2), 343 (1988)
4. D.M. Soares, O. Teschke, I. Torriani, J. Electrochem. Soc. **139**(1), 98 (1992)
5. N. Krstajic, M. Popovic, B. Grgur, M. Vojnovic, D. Sepa, J. Electroanal. Chem. **512**, 16 (2001)
6. V. Paserin, S. Marcuson, J. Shu, D.S. Wilkinson, Adv. Eng. Mater. **6**, 454 (2004)
7. S. Inazawa, A. Hosoe, M. Majima, K. Nitta, Sci. Technol. Rev **71**, 23 (2010)
8. E. Verlato, S. Cattarin, N. Comisso, A. Gambirasi, M. Musiani, L. Vazquez-Gomez, Electrocatal **3**, 48 (2012)
9. I. Bianchi, E. Guerrini, S. Trasatti, Chem. Phys. **319**, 192 (2005)

10. L. Vazquez-Gomez, S. Cattarin, P. Guerriero, M. Musiani, Electrochim. Acta **53**, 8310 (2008)
11. P. Kim, J.B. Joo, W. Kim, J. Kim, I.K. Song, J. Yi, J. Power Sources **160**, 987 (2006)
12. Y. Suo, I.M. Hsing, J. Power Sources **196**, 7945 (2011)
13. A. Dutta, S.S. Mahapatra, J. Datta, Int. J. Hydrog. Energy **36**, 14898 (2011)
14. R.M. Modibedi, T. Masombuka, M.K. Mathe, Int. J. Hydrog. Energy **36**, 4664 (2011)
15. B. Beyribey, B. Corbacioglu, Z. Altin, G. U. J. Sci. **22**(4), 351 (2009)
16. S.Y. Qian, B.E. Conway, G. Jerkiewicz, Int. J. Hydrog. Energy **25**, 539 (2000)
17. J.M. Skowroński, A. Czerwiński, T. Rozmanowski, Z. Rogulski, P. Krawczyk, Electrochim. Acta **52**, 5677 (2007)
18. J.K. Norskov, T. Bligaard, A. Logadottir, J.R. Kitchin, J.G. Chen, S. Pandelov, U. Stimming, J. Electrochem. Soc. **152**(3), J23 (2005)
19. T.H. Yang, S.I. Pyun, J. Electroanal. Chem. **414**, 127 (1996)
20. T.G. Kelly, S.T. Hunt, D.V. Esposito, J.G. Chen, Int. J. Hydrog. Energy **38**, 5638 (2013)
21. A. Pozio, S. Tosti, Handbook of Membrane Reactors: Reactor Types and Industrial Applications, Woodhead Publishing Ltd., Cambridge **16**, 607 (2013)
22. J. Banhart, Prog. Mater. Sci. **46**, 559 (2001)
23. B. Pierozynski, L. Smoczynski, J. Electrochem. Soc. **156**(9), B1045 (2009)
24. B. Pierozynski, Int. J. Electrochem. Sci. **6**, 63 (2011)
25. B. Pierozynski, Int. J. Hydrog. Energy **38**, 7733 (2013)
26. Z. Xie, P. He, L. Du, F. Dong, K. Dai, T. Zhang, Electrochim. Acta **88**, 390 (2013)
27. J.R. Macdonald, Electrochim. Acta **35**, 1483 (1990)
28. A. Prokopowicz, M. Opallo, Solid State Ionics **157**, 209 (2003)
29. L. Smoczyński, H. Ratnaweera, M. Kosobucka, M. Smoczyński, Sep. Purif. Technol. **122**, 412 (2014)
30. V. Pecharsky, P. Zavalij, *Fundamentals of Powder Diffraction and Structural Characterization of Materials, Springer, 2nd edition, New York*, 2009
31. T. Pajkossy, J. Electroanal. Chem. **364**, 111 (1994)
32. B.E. Conway, B. Pierozynski, J. Electroanal. Chem. **622**, 10 (2008)
33. A. Lasia, A. Rami, J Appl. Electrochem. **22**, 376 (1992)
34. L. Chen, A. Lasia, J. Electrochem. Soc. **138**, 3321 (1991)
35. M. Grdeń, M. Alsabet, G. Jerkiewicz, ACS Appl. Mater. Interfaces **4**, 3012 (2012)
36. J. van Drunen, B. Kinkead, M.C.P. Wang, E. Sourty, B.D. Gates, G. Jerkiewicz, ACS Appl. Mater. Interfaces **5**, 6712 (2013)
37. C. Hitz, A. Lasia, J. Electroanal. Chem. **500**, 213 (2001)
38. M.A. Dominguez-Crespo, A.M. Torres-Huerta, B. Brachetti-Sibaja, A. Flores-Vela, Int. J. Hydrog. Energy **36**, 135 (2011)
39. I. Herraiz-Cardona, E. Ortega, L. Vazquez-Gomez, V. Perez-Herranz, Int. J. Hydrog. Energy **37**, 2147 (2012)
40. J.G. Highfield, E. Claude, K. Oguro, Electrochim. Acta **44**, 2805 (1999)
41. R.K. Shervedani, A.R. Madram, Electrochim. Acta **53**, 426 (2007)
42. S. Martinez, M. Metikos-Hukovic, L. Valek, J. Mol. Catal. A Chem. **245**, 114 (2006)
43. B.E. Conway, in Modern Aspects of Electrochemistry, ed. by B.E. Conway, R.E. White, J.O'M. Bockris, Plenum Press, New York **16**, 103 (1985)
44. G.E. Badea, I. Maior, A. Cojocaru, I. Corbu, Rev. Roum. Chim. **52**(12), 1123 (2007)